

Multi-Epoch Observations of the Redwing Excess in the Spectrum of 3C279

Brian Punsly¹

ABSTRACT

It has been previously determined that there is a highly significant correlation between the spectral index from 10 GHz to 1350 Å and the amount of excess luminosity in the red wing of quasar CIV λ1549 broad emission lines (BELs). Ostensibly, the prominence of the red excess is associated with the radio jet emission mechanism and is most pronounced for lines of sight close to the jet axis. Studying the scant significant differences in the UV spectra of radio loud and radio quiet quasars might provide vital clues to the origin of the unknown process that creates powerful relativistic jets that appear in only about ten percent of quasars. In this study, the phenomenon is explored with multi-epoch observations of the MgII λ2798 broad line in 3C 279 which has one of the largest known redwing excesses in a quasar spectrum. The amount of excess that is detected appears to be independent of all directly observed optical continuum, radio or submm properties (fluxes or polarizations). The only trend that occurs in this sparse data is: the stronger the BEL, the larger the fraction of flux that resides in the redwing. It is concluded that more monitoring is needed and spectropolarimetry with a large telescope is essential during low states to understand more.

Subject headings: quasars: general — galaxies: active — quasars: emission lines — quasars: individual (3C 279)

1. Introduction

Perhaps the greatest mystery of the quasar phenomenon is that $\sim 10\%$ of the quasar population possess powerful relativistic radio jets (known generically as radio loud quasars RLQs). These are dramatic features that can transport $\gtrsim 10^{40}$ W hundreds of kiloparsecs into the intra-cluster medium (Willott et al. 1999). Yet, the majority of quasars are radio

¹1415 Granvia Altamira, Palos Verdes Estates CA, USA 90274 and ICRANet, Piazza della Repubblica 10 Pescara 65100, Italy, brian.punsly@verizon.net or brian.punsly@comdev-usa.com

quiet quasars (RQQs) that are defined by "weak" jet power. In spite of this most conspicuous property, the optical/UV continuum and broad emission lines (BELs) in RLQS and RQQs are remarkably similar (Corbin and Francis 1994; Zheng et al. 1997; Telfer et al. 2002). Systematic differences in the two families of spectra are only revealed by the study of subtle lower order spectral features (Corbin 1997b; Richards et al 2002). Perhaps the most extreme difference in the spectra of these two classes of objects is a highly significant correlation between the spectral index from 10 GHz to 1350 Å and the amount of excess luminosity in the red wing of quasar CIV λ1549 broad emission lines (BELs), at > 99.9999% statistical significance (Punsly 2010). The prominence of the redward excess is apparently associated with the radio jet emission mechanism and is most pronounced for lines of sight close to the jet axis.¹ In some blazars (core dominated radio sources), the asymmetry is so extreme that the line shape becomes similar to a right triangular, the emission is dominated by the red gently sloping side ("the hypotenuse"). In this paper, we explore why this effect is so pronounced in some radio loud AGN (active galactic nuclei) that are viewed along the jet axis.

The red excess in the BELs has been noted in anecdotal examples of blazar spectra including the first case to be studied in detail, Hα in 4C 34.47 in Corbin (1997a). The origin of the redwing excess is unknown and explanations have ranged from gravitational and transverse redshift within 200 M (gravitational radii) from the central black hole, reflection off optically thick, out-flowing clouds on the far side of the accretion disk or transmission through inflowing gas on the near side of the accretion disk (Corbin 1997a; Netzer et al. 1994; Marziani et al. 1996). None of these scenarios are substantiated, but are speculations that are designed to describe a difficult to understand observation. The archives of observational data seem inadequate for determining a likely explanation.

In Netzer et al. (1994), HST data were used to show that 3C 279 had very asymmetric CIV λ1549 and MgII λ2798 BELs. In this study, we explore the variation of the MgII λ2798 line profile over time in 3C 279. This is an interesting case study because 3C 279 is perhaps the most conspicuous blazar in the local Universe (z=0.5356 from Netzer et al. (1994)). It has the most extreme blazar properties, optical polarization larger than 20%, extreme variability in all observable bands, superluminal jet speeds exceeding 20c and it is one of the brightest gamma ray sources (Abdo et al. 2010; Ghisellini et al. 2010; Impey and Tapia 1990; Bonning et al. 2012; Larsson et al. 2012; Lister et al. 2009; Jorstad et al. 2011). 3C 279 also has a spectrum with some of the most redward asymmetric BELs ever observed. As

¹It should be noted that a subtlety of the correlation is that some lobe dominated quasars have significant asymmetry. The most extreme case in Figure 1 of Punsly (2010) is PKS 0454-020 with an asymmetry larger than most blazars.

a consequence of the extraordinary nature of this blazar, there is a wealth of simultaneous long term monitoring data from radio waves to gamma rays which facilitates multi-epoch comparisons. Since the effect is most pronounced in blazars, one is often forced to deal with the huge amount of dilution from the optical, high frequency tail of the Doppler enhanced synchrotron emission from the relativistic jet (Lind and Blandford 1985). Thus, in 3C 279 for example, it is difficult to extricate the BELs from the continuum unless the jet emission is weak (a low state).

2. Spectra From Three Epochs

The "Ground-based Observational Support of the Fermi Gamma-ray Space Telescope at the University of Arizona," Smith et al. (2009) provides an opportunity to find high signal to noise MgII $\lambda 2798$ spectra of 3C 279. The required combination of a weak synchrotron component and good seeing is not common, but with long term monitoring, the chance of a high signal to noise observation of the MgII $\lambda 2798$ BEL is vastly improved. The frequent monitoring with Steward Observatory also allows for the binning of data, thereby improving the signal to noise ratio in the redwing of the MgII $\lambda 2798$ BEL. Figure 1 plots the optical spectra at three distinct epochs, covering 18 years.

The first epoch is April 9, 1992. The blue frequencies are from the HST, Faint Object Spectrograph with the G400 grating. The longer wavelengths are from the 2.7 m telescope at the McDonald Observatory using the Large Cassegrain Spectrograph. These data were previously discussed in Netzer et al. (1994). The fully reduced and calibrated data were generously provided by B. Wills. The raw spectral data were tabulated every $\approx 0.35 \text{ \AA}$ and then binned and smoothed to a resolution of $\approx 1.4 \text{ \AA}$. The details of the data processing can be found in Netzer et al. (1994); Wills et al. (1995). The continuum during April 1992 was the brightest of the three epochs. Fortunately, the MgII $\lambda 2798$ BEL was very strong at this time. Other features to note are a similarly asymmetric CIV $\lambda 1549$ BEL from the same observing run with the G270 grating (not plotted, but see Netzer et al. (1994)) and a strong [OIII] $\lambda 5007$ narrow line.

The most recent epoch is the faintest, spanning the interval from April 7, 2010 to April 11, 2010. The data are from the 3m Bok Telescope of the Steward Observatory (Smith et al. 2009). The highest signal to noise epochs from this time interval were collected (and plotted in Figure 1) for future binning. The continuum in this state is an order of magnitude fainter than in 1992, and the asymmetric broad wing is clearly visible. Another interesting feature to note is the distinct [OII] $\lambda 3727$ narrow line. A second epoch from the Steward Observatory archive is a year earlier with a continuum luminosity intermediate between the other two

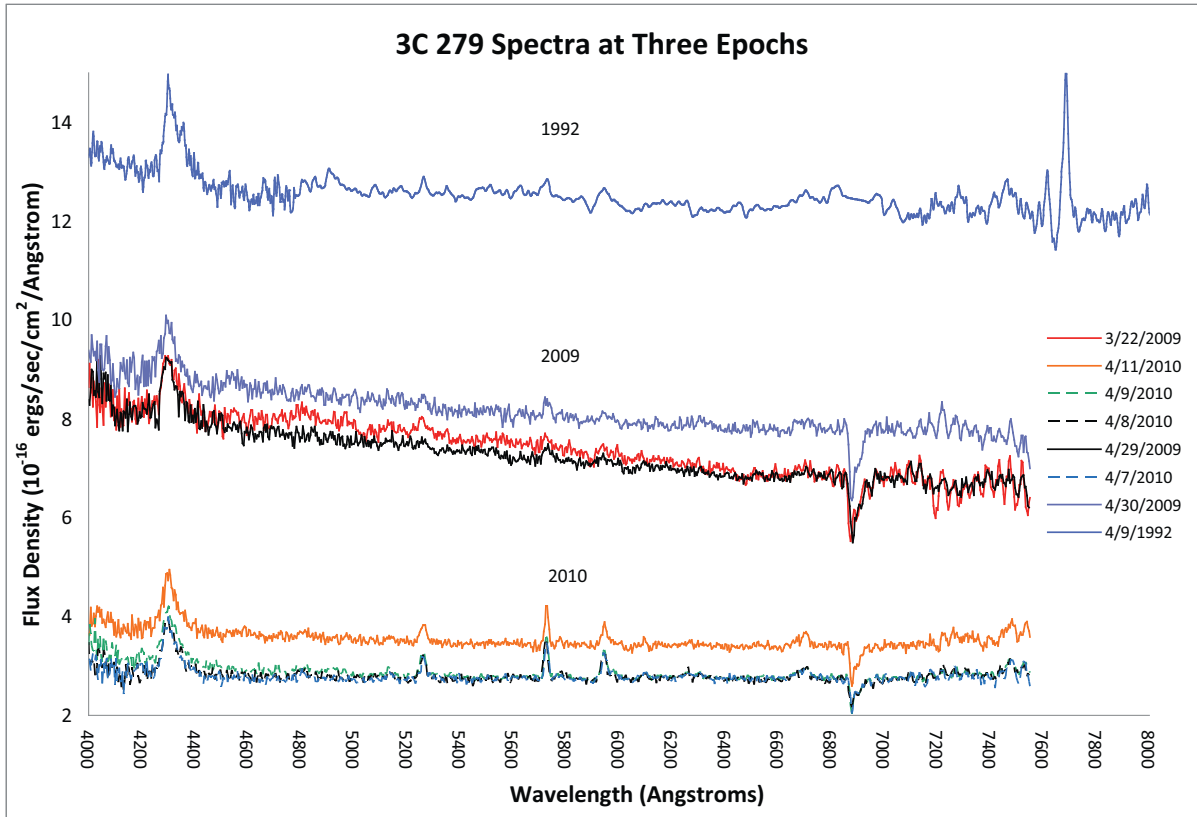


Fig. 1.— Optical spectra at three different epochs.

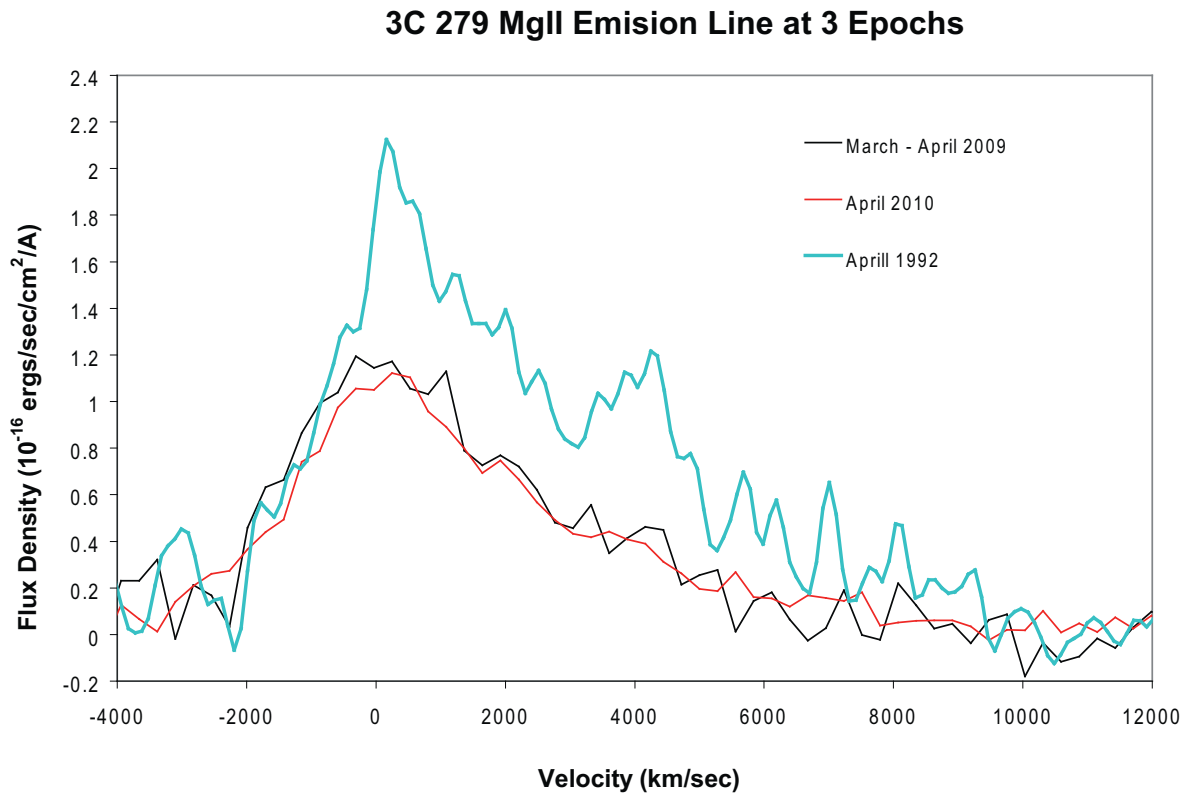


Fig. 2.— Comparison of MgII $\lambda 2798$ profiles in velocity space at three different epochs that are spread over 18 years.

epochs.

Figure 2 is a plot of the region of the spectrum that is contiguous to the Mg II BEL in velocity space. The line profiles are obtained after subtraction of a linear fit to the continuum from 4050 Å to 4750 Å. The HST data from B. Wills are not the data used to plot the Mg II line profile that was displayed in velocity space in Figure 2 of Netzer et al. (1994). That low resolution spectrum ($\sim 4\text{Å}$) was from a 15 minute observation with the 4m CTIO Telescope using the RC spectrograph 4 days later. The Steward Observatory line profiles were binned as a weighted average with a weight that is inversely proportional to the RMS noise in the adjacent continuum. Figure 2 indicates that the Mg II broad-line is virtually unchanged (within the accuracy of the observations) from 2009 to 2010, but drastically weaker than in 1992. This would seem to indicate a time scale for changes in the red wing excess that is larger than 1 year and less than 18 years. This is in contradistinction to jet emission that has order of unity variations on the orders of hours to weeks (Larsson et al. 2012). Thus, one does not expect to find trends between the amount of red excess and the rapid observed flux variations from the Doppler enhanced jet.

3. Characterizing the Red Asymmetry

In order to characterize the time variability in the MgII $\lambda 2798$ BEL depicted in Figure 2 requires a method of quantifying the redward line asymmetry. The amount of perceived red excess is not uniquely defined and three nonparametric methods for describing its magnitude are considered in Table 1.

The study in Wills et al. (1995) that included 3C 279 quantified the red asymmetry by A_{25-80} . The quantity, A_{25-80} , is defined in terms of the full width half maximum, FWHM, in Å, the midpoint of an imaginary line connecting a point defined at 1/4 of the peak flux density of the BEL on the red side of the BEL to 1/4 of the peak flux density on the blue side of the BEL, λ_{25} , and a similar midpoint defined at 8/10 of the flux density maximum, λ_{80} , as

$$A_{25-80} = \frac{\lambda_{25} - \lambda_{80}}{FWHM}. \quad (1)$$

A positive value of A_{25-80} means that there is excess flux in the red broad wing of the BEL. A negative value of A_{25-80} indicates a blueward asymmetry of the BEL. In order to calculate A_{25-80} in the presence of the random noise that is superimposed on the line profiles in Figure 2, one can proceed as in Wills et al. (1995). Using the continuum fit described in the last section, the lines are fit by two or three Gaussians profiles which interpolates between the fluctuations of the random noise. The values for each epoch are listed in column (5) of Table

1.

The errors associated with estimating A_{25-80} arise primarily from the uncertainty in λ_{25} since the signal to noise ratio is the smallest in the broad wings. The error in each quantity in equation (1) was individually estimated and the results were added in quadrature. The error in λ_{25} , for example, was achieved by approximating the region near the 1/4 maximum point of the line profile by the composite Gaussian fit. The error in λ_{25} was the determined to be slope of this composite Gaussian fit ($\partial\lambda/\partial F_\lambda$) at the 1/4 maximum point times the RMS noise level. This naturally produces larger errors in A_{25-80} for epochs with very broad wings, i.e., the more horizontal the spectrum in the wings, the larger the slope ($\partial\lambda/\partial F_\lambda$) will be. These uncertainties are listed in column (5) of Table 1.

The line luminosities in Table 1 are computed using the Galactic extinction from Schlafly and Finkbeiner (2011) as posted in the NASA Extragalactic Database and a cosmological model defined by $H_0=70$ km/s/Mpc, $\Omega_\Lambda = 0.7$ and $\Omega_m = 0.3$. The first thing to notice is that the 2009 and 2010 line profiles are virtually identical in Figure 2 and Table 1 even though the optical polarization is an order of magnitude larger in 2009. The line was decomposed into two empirical components, a blue side (with negative velocity in Figure 2) and a red side based on a redshift, $z = 0.5356$. Column (2) of Table 1 is the total line luminosity, $L(\text{MgII})$, and column (3) is the ratio of red side luminosity, $L(\text{MgII})_{\text{red}}$, to the blue side luminosity, $L(\text{MgII})_{\text{blue}}$. Column (4) is the red excess that is defined by reflecting the blue side about the zero velocity axis and computing the red residuals. This quantity is then normalized by $L(\text{MgII})$,

$$\text{Red Excess} \equiv \frac{L(\text{MgII}) - 2L(\text{MgII})_{\text{blue}}}{L(\text{MgII})}. \quad (2)$$

The next column is the asymmetry parameter, A_{25-80} , defined in Equation (1). The last two columns depict the strength and polarization of the optical continuum.

The errors in column (2) of Table 1 represent the luminosity of the RMS of the residuals (noise level) to the composite Gaussian fit that is obtained by integrating the residual luminosity over the entire line profile from -5,000 km/sec (blue) to 13,000 km/sec (red). Similarly, one computes the uncertainty in the blue (red) side of the line decomposition as

Table 1: Mg II Emission Line and Optical Continuum Properties

Epoch	$L(\text{MgII})$ (10^{43} erg/s)	$\frac{L(\text{MgII})_{\text{red}}}{L(\text{MgII})_{\text{blue}}}$	Red Excess	A_{25-80}	6500 Å Flux Density (ergs/ cm ² /s/ Å)	Continuum Polarization
1992	1.78 ± 0.31	2.34 ± 0.58	0.40 ± 0.07	0.55 ± 0.12	1.32×10^{-15}	...
2009	0.96 ± 0.28	1.56 ± 0.48	0.22 ± 0.05	0.24 ± 0.13	8.44×10^{-16}	10.1 % - 21.1 %
2010	0.96 ± 0.15	1.47 ± 0.26	0.19 ± 0.03	0.27 ± 0.07	2.92×10^{-16}	1.4 % - 2.9 %

the integrated luminosity of the RMS residual noise level (note that the RMS residual noise level is always positive, by definition, even when the residual luminosity is neagtive) over the blue (red) portion of the line profile from -5,000 km/sec to 0 km/sec (0 km/sec to 13,000 km/sec). The errors in the blue and red sides propagagate through quadratures to generate the error estimates in columns (3) and (4).

The intent of presenting Table 1 is to demonstrate that the variation in the red wing excess over an 18 year time span exists independent of how it is defined. The last two rows show that a virtually unchanged line profile can still be clearly detected even when the synchrotron background triples in strength. Thus, the Steward Observatory monitoring can detect a well-defined asymmetric profile over a wide range of continuum luminosity and should provide a wealth of epochs with asymmetric profiles in the coming years. The preliminary trend in the data is that when the line strength is elevated, the degree of asymmetry increases.

4. Discussion

The purpose of this Letter was not to make strong claims as to the physical origin the of red wing excess in blazars. The purpose is to show that it is possible to see changes in the red wing excess in blazars.

The primary result of Table 1 is that the MgII redwing excess does not vary in consort with the rest of the broad line emission. Considering the conspicuous jet viewed in a nearly pole-on orientation, it seems likely that the red excess is associated with the jet and not the virialized gas responsible for the core and blue wing of the emission line. This seems to favor the optically thick outflow scenario described in the introduction. The phenomenon might be related to the outflow that is responsible for the broad absorption lines seen in some polar orientation broad absorption line quasars (Zhou et al. 2006; Ghosh and Punsly 2007; Punsly and Zhang 2010).

Temporal variations in line properties can be the compared to contemporaneous variations of jet properties on subparsec scales that can be detected during the extensive monitoring from millimeter wavelengths to gamma rays of many FERMI selected blazars and high frequency (43 GHz) VLBA images (Ataraski et al. 2011; Bonning et al. 2012; Jorstad et al. 2011; Larsson et al. 2012). In principle, any such causal connections can be be used as a probe of possible relationships between jet propagation/formation and the gaseous environment on subparsec scales, the broad line region. This comment in one way attempts to minimize the complexities introduced by large Doppler enhancement of the emission that

can make it extremely difficult to determine intrinsic properties of the jet.

The data presented here from three epochs observed with modest apertures are insufficient to properly explore the possibilities noted above. To improve our understanding requires more optical data with larger telescopes and long term monitoring. Future long term monitoring (since the time scale for variation is longer than one year from Table 1) of the FWHM and the luminosity using the decompositions into red, blue and core components can be used as a crude surrogate for reverberation mapping of the red wing (since the optical continuum is hidden by the synchrotron emission). It would be important to find time lags (if any) between the blue wing, the line core and the red excess. This would yield information on the relative locations of the gas producing the line core and the gas responsible for the red excess. Perhaps of more interest, it is proposed that the Steward Observatory monitoring be used as a trigger for a large telescope observation. If a broad line is clearly displayed in the Steward Observatory data this would trigger a large (8m) telescope to observe 3C 279 with high resolution spectropolarimetry. The purpose being the same as in the study of broad absorption line quasars, to look for signs of scattered emission in the red wing: position angle rotation or a change in the polarization level (Smith et al. 1995; Ogle 1997). These data could be used as a probe of the geometry in scenarios that the red wing is scattered emission that was resonantly absorbed in an out-flowing wind or it is scattered light from an optically thick "moving mirror" that is created by a stream of clouds in motion.

I am indebted to Bev Wills for sharing the reduced HST data from 1992 and her ground based data from the same campaign. I would like to thank Matt Malkan for sharing his expertise and encouraging me to pursue this topic. Data from the Steward Observatory spectropolarimetric monitoring project were used. This program is supported by Fermi Guest Investigator grants NNX08AW56G, NNX09AU10G, and NNX12AO93G. I was also very fortunate to have a referee who greatly improved the clarity and focus of this effort.

REFERENCES

- Abdo, A. et al. 2010, ApJ **722** 520
Ataraski, J. 2011, A & A **536** A15
Bonning, E. et al. 2012, ApJ **756** 13
Corbin, M. 1997, ApJ **485** 517
Corbin, M. 1997, ApJS **113** 245

- Corbin, M. and Francis, P. 1994, AJ **108** 2016
- Ghisellini, G. et al. 2010, MNRAS **402**, 497
- Impey, C. and Tapia, S., 1990 ApJ **354** 124
- Jorstad, S., Marscher, A., Agudo, I., Harrison, B. 2011 Fermi Symposium proceedings - eConf C110509 <http://xxx.lanl.gov/abs/1111.0110>
- Ghosh, K. and Punsly, B. 2007 ApJL **661** 139
- Larsson, J. et al., (2012) 2012 Fermi & Jansky Proceedings - eConf C1111101 <http://arxiv.org/abs/1206.3799v1>
- Lind, K., Blandford, R. 1985, ApJ **295** 358
- Lister, M. et al 2009, ApJL **696** 22
- Marziani, P. et al 1996, ApJS **104** 37
- Netzer, H., Kazanas, D., Baldwin, J., Ferland, G., Browne, I.W.A. 1994, ApJ **430** 191
- Ogle, P. 1997 in ASP Conf. Ser. 128, **Mass Ejection from Active Nuclei** ed, N.Arav, I.
- Punsly, B. 2010, ApJ **713** 232
- Punsly, B. and Zhang, S. 2010 ApJ **725** 1928
- Richards, G. et al 2002, AJ **124** 1
- Schlaafy, E., Finkbeiner, D. 2011, ApJ **737** 103
- Smith, P. et al. 1995, ApJ **444** 146
- Smith, P., Montiel, E., Rightley, S., Turner, J., Schmidt, G.D., Jannuzi, B.T 2009, arXiv:0912.3621 2009 Fermi Symposium, eConf Proceedings C091122 and <http://james.as.arizona.edu/~psmith/Fermi/>
- Telfer, R., Zheng, W., Kriss, G., Davidsen, A. 2002, ApJ **565** 773
- Willott, C., Rawlings, S., Blundell, K., Lacy, M. 1999, MNRAS **309** 1017
- Wills, B. et al 1995, ApJ **437** 139
- Zheng, W. et al 1997, ApJ **475** 469

Zhou, H. et al 2006 ApJ **639** 716